International Journal of Automotive Technology, Vol. 22, No. 1, pp. 11–18 (2021)
DOI 10.1007/s12239–021–0002–x

pISSN 1229–9138/ eISSN 1976–3832

STUDY ON CAVITATING FLOW INSIDE ORIFICE AND SPRAY ANGLE NEAR NOZZLE TIP ACCORDING TO THE POSITION OF NEEDLE USING ENLARGED TRANSPARENT ACRYLIC NOZZLE

Byunggyun Kim[1), 4)], Seungcheon Ro[2), 5)], Suhan Park[3)*], Young-Bae Kim[3)], Byungchul Choi[3)], Seunghun Jung[3)] and Dong-Weon Lee[3)]

[1)]Department of Mechanical Engineering, Graduate School of Chonnam National University, Gwangju 61186, Korea
[2)]National Institute of Environmental Research, 42 Hwangyeong-ro, Seo-gu, Incheon 22689, Korea
[3)]School of Mechanical Engineering, Chonnam National University, Gwangju 61186, Korea
[4)]Powertrain Control & Tuning Team, Renault Samsung Motors, 61 Tapsil-ro, Giheung-gu, Yongin-si, Gyeonggi-do 17084, Korea
[5)]Product Design Team 2, Hyundai-Kefico, 102 Gosan-ro, Gunpo-si, Gyeonggi-do 15849, Korea

(Received 27 May 2019; Revised 10 October 2019; Accepted 17 January 2020)

ABSTRACT–This study aims to analyze effect of needle position inside nozzle on the internal and external flow characteristics. To visualize cavitating flow inside nozzle, the transparent acrylic nozzle was used. We tested five needle positions that simulated the needle movement of injector. The cross-section of test nozzle is rectangular with a very narrow width instead of circular shaped for a better visualization of cavitating flow. The inside of the nozzle was visualized by the shadowgraphic visualization using a high-speed camera and a metal-halide lamp. From the experiments, development of the cavitating flow according to the needle positions depends on the flow velocity and the cavitation number. The cavitation length, cavitation width, and spray angle are relatively symmetrically shown when the needle was at the center. However, they were asymmetrical when the needle position was biased. When the needle positions were in the same on the vertical line, the minimum cavitation length, minimum cavitation width, and minimum spray angle were larger when the upper level. The needle position affects the development timing and cavitation growth. When the needle position was located at the upper level, the hydraulic flip occurred at a higher injection pressure than the lower level.

KEY WORDS : Cavitation, Cavitation length, Cavitation width, Needle position, Spray angle, Shadowgraphic visualization

NOMENCLATURE

L : length
W : width
H : height
θ : spray angle
Re : reynolds number
σ : cavitation number
C_d : discharge coefficient
ρ : density
V : velocity
Q : flow rate
ΔP : nozzle injection pressure
P : pressure
υ : kinematic viscosity

SUBSCRIPTS

inj : injection
cav: cavitation
w : water
v : vapor
a : atmospheric

1. INTRODUCTION

Regulation of harmful exhaust gas emitted from automobiles equipped with an internal combustion engine is gradually being strengthened. To satisfy the exhaust emission regulations, the development of after-treatment equipment such as a diesel particulate filter (DPF), selective catalyst reduction (SCR), and improvement of the combustion performance in the combustion chamber are being studied actively. Combustion and exhaust gas generation in the internal combustion engine are significantly influenced by the fuel–air mixture formation characteristics in the combustion chamber, and the mixer is

*Corresponding author. e-mail: suhanpark@jnu.ac.kr

influenced by the atomization characteristics of the fuel. Therefore, spray optimization of the fuel injected from the injector is one of the important strategies to improve the thermal efficiency of the engine and to reduce the exhaust emission of the internal combustion engine.

In recent years, to form a uniform mixture and improve atomization, the injection pressure is increased and the size of the injector holes is gradually reduced (Moro *et al.*, 2017; Salvador *et al.*, 2017; Valera-Medina *et al.*, 2017). Therefore, cavitating flow inside the injector nozzle orifice is inevitable. The cavitating flow is affected by the vena-contracta formation with a narrow flow cross-sectional area downstream of the injector, as the fluid enters the nozzle orifice inlet and rapidly decreases in the cross-sectional area and does not flow along the shape. Also, the velocity increase in the fluid due to the reduction of the flow cross-sectional area and the formation of the low-pressure area are the main causes of the formation of the cavitating flow. Consequently, the pressure at the inlet of the nozzle becomes a vertical gradient of the flow, and the pressure is the smallest at the orifice wall (Potter and Wiggert, 2002). Hence, the fluid pressure drops below the saturation vapor pressure near the nozzle wall, causing cavitation. Understanding the cavitation phenomenon is essential because the cavitating flow inside the injector nozzle is critical in spray and atomization.

Bergwerk (1959) conducted a flow experiment using an injector of diameter 0.2 ~ 2.5 mm and indicated that the cavitating flow inside the injector nozzle was a major factor in determining the spray atomization characteristics. Sou *et al.* (2007), Prasetya *et al.* (2015), Bicer and Sou (2015) conducted extensive research on cavitating flow using a two-dimensional (2D) single-hole acrylic nozzle. They reported that the change of the nozzle geometry significantly affects the cavitating flow and the cavitating flow influences the spray characteristics such as the spray angle and the ligament formation. Chaves *et al.* (2008) fabricated an acrylic nozzle of the size used in a real diesel injector and studied the velocity field change due to cavitation generation using particle image velocimetry (PIV) measurements. Leng *et al.* (2018) investigated the effects of V-type intersecting hole on cavitating flow and near-field flow dynamics. They reported that the use of V-type intersecting hole eliminated the generation of cavitation inside the nozzle orifice, and increase the discharge coefficient. Ebrahimi *et al.* (2017) studied the fundamental study for cavitating flow, and suggested new theoretical corrections suitable for high-pressure conditions. Park *et al.* (2008) compared the spray characteristics and cavitation characteristics of biodiesel and diesel fuel using enlarged transparent acrylic nozzles. Suh and Lee (2008) investigated spray atomization characteristics using enlarged transparent acrylic nozzles with different length and width ratios. In the cavitating flow, the Sauter mean diameter (SMD) values of the axial and radial direction were smaller than the Sauter mean diameter of the turbulent flow. Recently, Duke *et al.* (2013, 2015, 2016) developed the measurement method of cavitating flow inside nozzle using X-ray technique. They measured the distribution of cavitation bubbles using very small nozzles of 500 μm, and found that wall-generated bubbles were separated and accumulated along the nozzle centerline, respectively.

As described above, although various studies on cavitation using enlarged transparent acrylic nozzles and real-size nozzles have been performed, studies on the relationship between cavitation and spray characteristics have not yet been clarified. In particular, the effect of the needle position on the cavitating flow and spray characteristics in the 2D single-hole nozzle has not been clearly understood. The eccentricity of the needle in the injector during fuel injection was primarily studied through computational fluid dynamics (CFD) analysis, and was found to affect the spray characteristics (Salvador *et al.*, 2014; Wang *et al.*, 2018). That is, when the injector needle is opening or closing to inject fuel from a gasoline or diesel injector, it does not move in a straight line. This phenomenon affects the fluid flow and turbulence intensity in the upper region of the orifice inlet. As a result, this phenomenon affects the occurrence of cavitation, and the spray angle is also affected.

Therefore, in this study, we investigated how the internal flow characteristics of the nozzle orifice, cavitation length, cavitation width, and the external flow characteristics of the spray angle and jet flow, are influenced by the needle positions.

2. EXPERIMENTAL APPARATUS SET-UP AND PROCEDURE

2.1. Experimental Apparatus

Figure 1 is a schematic of the apparatus for visualizing the cavitating flow inside the nozzle. Water was used as the working fluid. Water was supplied to the nozzle at 0.1 bar using an inverter pump, and the flow rate was measured with a turbine type flow meter (BF50, Nuriteck). The water passing through the acrylic nozzle was stored in the nozzle reservoir tank and the water was moved back to the inverter pump (PBI-205MA, Wilo) reservoir tank through the underwater pump (Pd-G050M, Wilo) to establish the circulation system.

The internal or external flow was visualized using a metal–halide lamp (MID-25FC, 250W) light source and a high-speed camera (FASTCAM, Mini AX100). The sensitivity of the high-speed camera is ISO 40,000 for monochrome, ISO 16,000 for color, and the shutter speed is adjustable from 1.05 μs to 1 ms. The maximum resolution can be up to 4,000 frame per second (FPS) based on 1024 × 1024 pixels, and the minimum resolution is up to 540,000 FPS based on 128 × 16 pixels. Macroscopic spray and cavitating flow images were taken using 105 mm SIGMA lens and Extension tube. The high-speed camera was placed in front of the nozzle, and the light source was installed behind the nozzle. In addition, cavitation was visualized using the shadowgraph technique by placing the filter paper between the acrylic nozzle and the metal–halide lamp. The acquired images were analyzed using

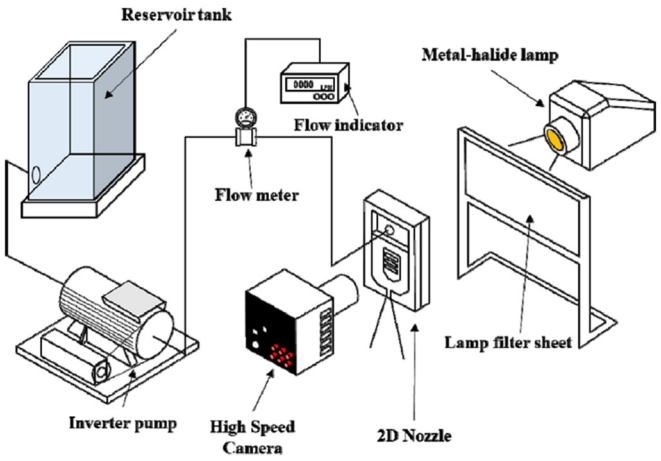

Figure 1. Schematic diagram of experimental setup.

a self-produced image processing program. The contents and methods of analysis are described in detail in section 2.2.

Figure 2 shows the schematic of 2D nozzle and the needle positions. The nozzle was set to a length (L) of 8 mm, width (W) of 4 mm and height (H) of 4 mm. The nozzle width was set to 4 mm due to limitations in manufacturing technology and convenience of visibility, and target nozzle configuration was set to base on the nozzle width. That is, we kept nozzle height the same as the nozzle width, so that the cross section of the nozzle passage through which the working fluid passed was square. To simulate the needle motion when injecting fuel from a diesel or gasoline injector, the needle positions were set to upper left and lower left, upper right and lower right, and

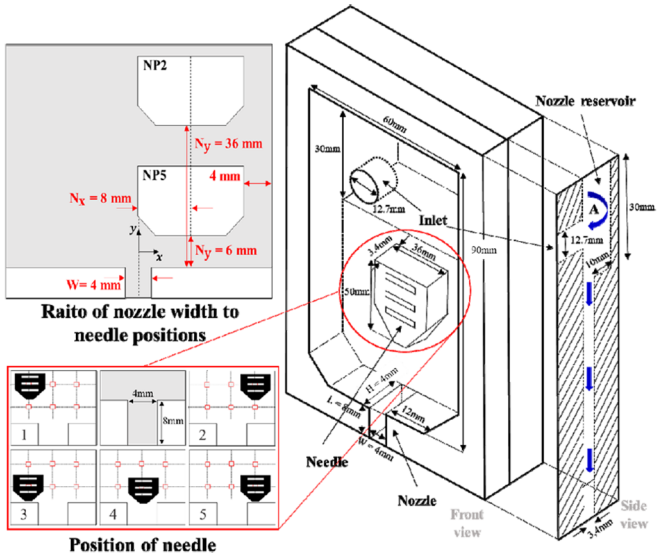

Figure 2. Schematic of 2D nozzle (length to width ratio = 2) and needle positions.

center. However, to confirm a clear change in the internal and external flow depending on the needle position, the diesel injector needle motion was referenced. Also, the distance between the needle positions is exaggerated compared to the actual injector. The needle positions were based on the nozzle width (W = 4 mm). When the needle maximum position, N_x/W was 2.0. When the needle position set to start of end or injection, needle lift was set to N_y/W = 1.5. Also, when the needle position set to the maximum needle lift during fuel injection, needle lift was set to N_y/W = 9.0. N_x is the distance between the centers of the needle and nozzle and N_y is the distance between the bottom of the needle and the nozzle seat. Details are shown in the upper left corner of Figure 2. In Figure 2, the nozzle reservoir (A) is designed to prevent the turbulent intensity changes due to swirling and tumbling from affecting the cavitation generation and development as much as possible because the fluid flows vertically into the nozzle. The nozzle reservoir had a width of 60 mm, height of 30 mm, and depth of 10 mm.

2.2. Analysis Methods

Figure 3 shows the image processing method, the cavitation length (L_{cav}), the cavitation width (W_{cav}), and the spray angle (θ). The first image obtained by the shadowgraphic technique delineates only the nozzle part where the cavitation occurred and the external flow part, and removed the background of the cropped image. Subsequently, the black and white processing, binarization processing, and filter processing were performed.

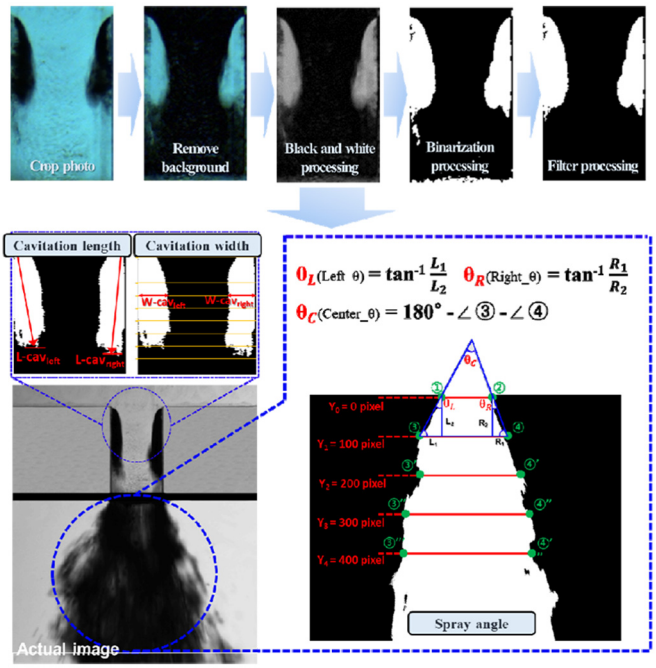

Figure 3. Image processing methods and definitions of cavitation length (L_{cav}), cavitation width (W_{cav}), and spray angle (θ).

The cavitation length is subsequently defined as the farthest distance from the incipient cavitation, and the cavitation width is defined as the maximum distance from the nozzle wall to the cavitation measured at each line, after defining an arbitrary line at equal intervals from the nozzle inlet to the nozzle outlet. Sato and Saito (2002) explained that a cavitation cloud peeled off from the primary cavitation was generated with a cycle, indicating a shedding phenomenon. In this experiment, the cavitation length and width were measured without considering the shedding phenomenon due to cavitation clouds. The spray angle was calculated using the equation shown in Figure 3 with four points generated at the end of the nozzle (y_0) and the 100 pixel point (y_1, about 2 mm). Subsequently, the four spray angles generated at the nozzle outlet end (y_0), and at the 200 pixel (y_2, about 4 mm), 300 pixel (y_3, about 6 mm), and 400 pixel (y_4, about 8 mm) points were added and the average value was used.

Since the cavitating flow is transient state, it is difficult to measure the data in a steady state. Therefore, the values of spray angle, cavitation width, and cavitation length were acquired with when the cavitating flow was judged to be in quasi-equilibrium based on the flow rate and pressure. Then, 100 images of 7200 images (7200 FPS) were acquired using a high-speed camera, and the average value of the acquired 100 image values of each side (left side nozzle, right side nozzle) was used. Equations (1) to (3) were obtained using the fluid flow rate, injection pressure, and fluid properties measured in this experiment. The three dimensionless numbers in the equation are the Reynolds number (Re), the cavitation number (σ), and the discharge coefficient (Cd).

$$\text{Reynolds number : } Re = VD/\upsilon \tag{1}$$

$$\text{Cavitation number : } \sigma = \frac{P_a - P_v}{0.5\rho_w V^2} \tag{2}$$

$$\text{Discharge coefficient : } Cd = \frac{Q}{A\sqrt{2\Delta P/\rho_w}} \tag{3}$$

The cavitation number is expressed as the ratio of the static pressure ($P_a - P_v$) to the dynamic pressure ($0.5\rho_w V^2$) of the flowing fluid derived from the Bernoulli equation. An increase in the cavitation number means a decrease in the cavitation generation and intensity, and a decrease in the cavitation number means an increase in the cavitation generation and strength. Therefore, theoretically, the generation and strength of the cavitation can be controlled by controlling the static pressure and the fluid flow rate. The flow characteristics of the nozzle were compared and analyzed through the correlation analysis between the cavitation number/Reynolds number and injection pressure/discharge coefficient. The velocity (V) of the fluid is the value obtained by dividing the cross-sectional area (Q = AV) of the nozzle at the measured flow rate (Q), and the characteristic length value used in the Reynolds number is the hydraulic diameter. P_v, P_a, and ΔP denote the vapor pressure, atmospheric pressure, and nozzle pressure, respectively. υ and ρ_w denote the dynamic viscosity and density of water, respectively. The experimental conditions and the physical properties of the fluid are shown in Table 1.

Table 1. Experimental condition and fluid properties.

Item	Specification
Working fluid	Liquid (water)
Injection pressure	1.0–3.9 bar
Reynolds number (Re)	22,000–39,000
Cavitation number (σ)	0.9–2.8
Ambient pressure	1.0 bar
Ambient temperature	278 K (Room temperature)
Dynamic viscosity	1.52×10^6 m^2/s
Density	998.2 kg/m^3

3. RESULTS AND DISCUSSION

3.1. Nozzle Inside and Outside Flow Characteristics

Figure 4 shows the development of the cavitation inside the nozzle and the jet flow by changing the needle position. Cavitation was observed for all needle positions with the steps of "Inception cavitation," "developing cavitation," "supercavitation," and "hydraulic flip." As shown in Figure 4, cavitation can be classified as "Inception cavitation" at V = 9.06 m/s to 9.16 m/s, σ = 2.29 to 2.45; "developing cavitation" at V = 10.94 m/s to 11.25 m/s, σ = 1.59 to 1.68; "super cavitation" at V = 11.87 m/s to 12.6 m/s, σ = 1.26 to 1.42; "hydraulic flip" at V = 10.83 m/s to 11.56 m/s, σ = 1.51 to 1.71.

These results show that the generation and development of cavitation under the current experimental conditions are affected not by the needle position but by the velocity. Further, as the injection pressure increased, the jet flow became more intense and the spray angle increased as the cavitation growth progressed closer to the nozzle outlet region. Subsequently, when the injection pressure is sufficiently increased to cause the hydraulic flip, the spray angle is drastically decreased and the jet flow is stabilized. This is because when the cavitation is generated, the fluid flow is reattached to the nozzle wall surface after leaving the cavitation area. At this time, vertical momentum in the flow direction of the local region occurring at the end of the cavitation increases the spray angle because it affects the fluid flow. Therefore, as shown in Figure 4, in the super cavitation, the flow is most affected by the momentum, and the spray angle is the largest. However, the reason for the dramatic decrease in the spray angle in the hydraulic flip region is that, because the fluid is not reattached to the nozzle wall, unlike the super cavitation, the vertical momentum in the flow direction of the local region occurring at the end of the cavitation is not formed (Sou *et al.*, 2015).

Meanwhile, cavitating flow developed in different depending on the needle positions. When the needle position was in the

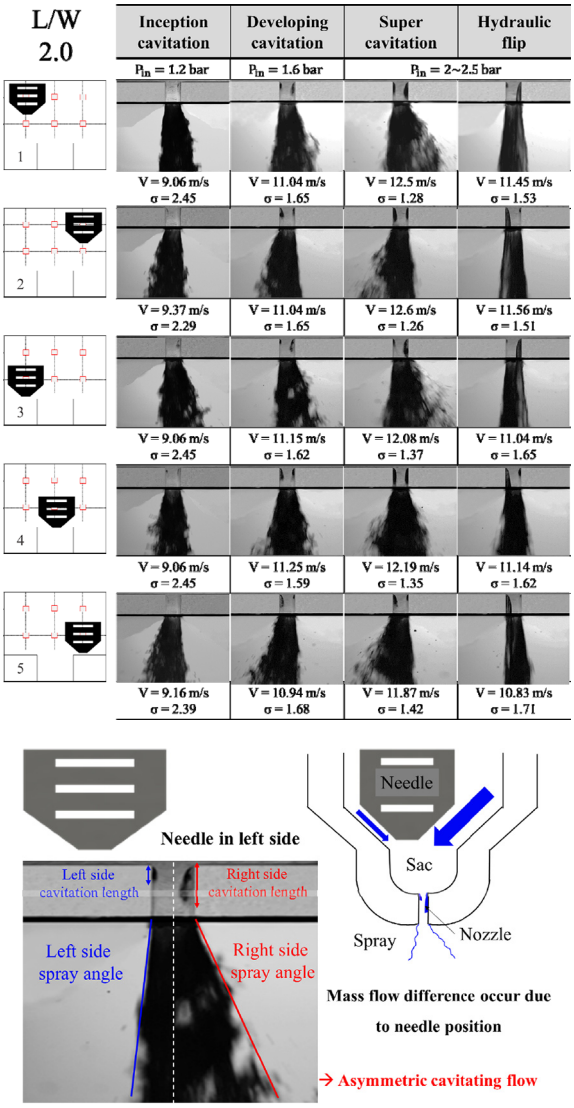

Figure 4. Cavitation and jet flows in the length-to-width ratio = 2.0 nozzle according to needle positions.

middle, cavitation was developed relatively symmetrically. However, the cavitation length, cavitation width, and spray angle were asymmetric when the needle position was biased. This is because when the needle position is biased, the flow rate is relatively decreased compared to the region where the flow path of the narrowed from the both wall surfaces is widened. This asymmetric flow continues to the nozzle inlet, resulting in an asymmetrical generation and development of cavitation. That is, when the needle positions are biased, the vena-contracta occurs asymmetrically on the left wall or the right wall of the nozzle owing to the velocity difference of the fluid, hence the asymmetric cavitation phenomenon (Suh and Lee, 2008). The latter is attributed to the cavitation length, cavitation width, and spray angle, shown in Figure 4.

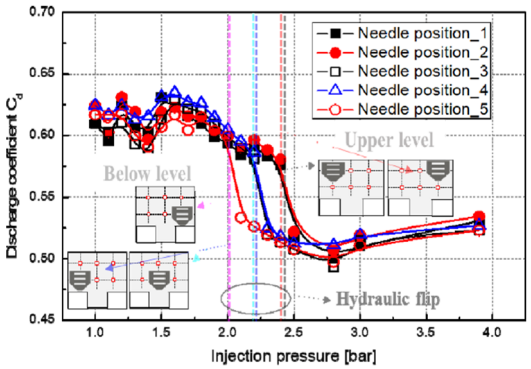

Figure 5. Relationship between injection pressure - discharge coefficient.

3.2. Relationship between Needle Position and Discharge Coefficient

Figure 5 shows the relationship between injection pressure and discharge coefficient according to the needle position. Regardless of the needle position, the discharge coefficient increases and decreases periodically at the injection pressure of 1.0 ~ 1.5 bar. This appears to be due to the irregular development of cavitating flow at the injection pressure interval. In the 1.5 ~ 2.0 bar section, the discharge coefficient is decreased and the discharge coefficient is decreased rapidly at the injection pressure range of 2.0 bar or higher, which corresponds to the hydraulic flip. It is considered that the flow resistance is generated more than the cavitation generation and development region because the cavitation is formed up to the nozzle outlet in the hydraulic flip and the flow effective area is decreased. Additionally, a difference in the injection pressure point where the discharge coefficient decreases depending on the needle position is shown. If the needle is located at the upper level (needle positions 1, 2), the discharge coefficient decreases later because of the hydraulic flip at relatively higher pressures. If the needle is located the lower level (needle positions 3, 4, 5), the hydraulic flip occurs at a relatively lower pressure and the discharge coefficient decreases more quickly. This is because, when the injection pressure is the same, the flow rate at the nozzle inlet region when the needle is located the lower level (needle positions 3,4,5) is relatively decreased as compared with the case where the needle is located at the upper level (needle positions 1, 2). Therefore, the influence of the pressure at the nozzle inlet region is considered as relatively larger when the flow rate is smaller than when the flow rate is larger. Consequently, the hydraulic flip is considered to occur more quickly.

3.3. Comparison of Cavitation Length, Cavitation Width, and Spray Angle according to Needle Position

Figure 6 shows the relationship between injection pressure and dimensionless cavitation length depending on needle position. The dimensionless cavitation length is the length of the

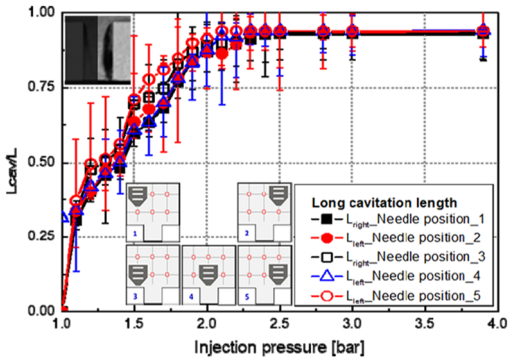

(a) Long cavitation length depending on needle position

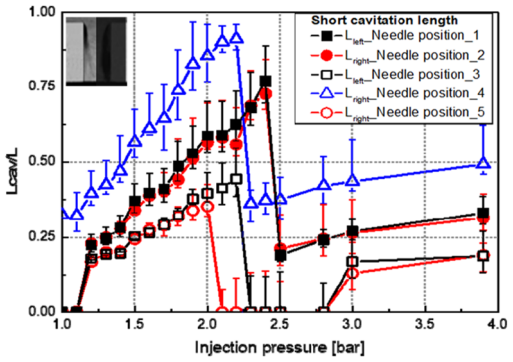

(b) Short cavitation length depending on needle position

Figure 6. Effect of needle position on dimensionless cavitation length on both sides of the nozzle.

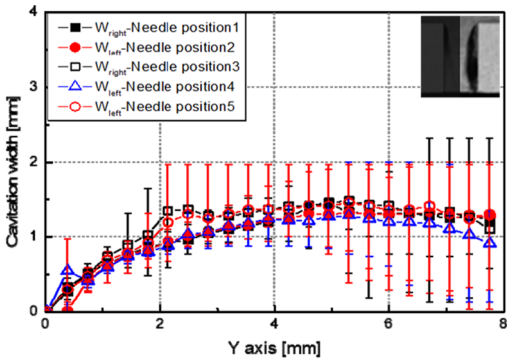

(a) Large cavitation width depending on needle position

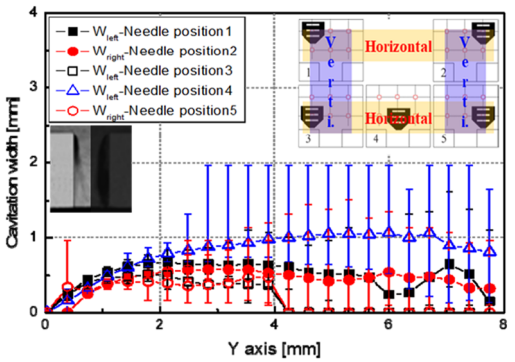

(b) Small cavitation width depending on needle position

Figure 7. Effect of needle position on cavitation width on both sides of the nozzle.

developed cavitation divided by the orifice length. From the definition of the cavitation number, as the injection pressure increases, the flow velocity of the fluid inside the orifice increases and thus the cavitation length becomes increased. However, unlike when the needle position is symmetrical, if the needle is biased to one side, the cavitation length grows asymmetrically. Figure 6 (a) shows the long part of the asymmetric cavitation length as the needle position changes. Regardless of the needle position, the cavitation length grows at a similar trend. However, the cavitation length is confirmed to be long on the opposite side of the biased needle position. Figure 6 (b) is a graph showing the short part of the asymmetric cavitation length depending on needle position. Unlike the case where the cavitation length was long, the tendency is consistent; however, a difference is shown between the development timing and the growth degree of the cavitation. The cavitation length is confirmed to be short on the same side of the biased needle position. In addition, when the needle positions are located at the upper level (needle positions 1, 2), and the lower level (needle positions 3,5), the maximum dimensionless cavitation lengths increased to 0.75, and 0.3 to 0.5, respectively; therefore, the cavitation lengths are longer when the needle is located at the upper level. The hydraulic flip was occured at relatively higher injection pressure when the needle position was upper level (2.4 ~ 2.5 bar) compared to lower level (2.0 ~ 2.3 bar). The needle position is shown to affect the asymmetry formation of the cavitation and the occurrence degree of the hydraulic flip. Likewise, Figure 6 shows that the flow rate at the region where the needle is not located is relatively smaller than that at the region where the needle is located, thus affecting the inlet region of the nozzle. Further, the cavitation length is converged to 1.0 because the cavitation is relatively symmetrically generated when the needle is located at the center.

Figure 7 shows the cavitation width according to the needle position and nozzle length(Y-axis). The cavitation width was measured immediately prior to the occurrence of hydraulic flip, so the injection pressure is different according to the needle position. The cavitation width was the average value of each measured width values at a specified position (divided into 18 equal intervals from the orifice inlet to the outlet.) in the manner defined in section 2.2. The cavitation width also developed relatively symmetrically when the needle position is in the center, but it grows asymmetrically if the needle position is biased. Figure 7 (a) is a graph showing the thick side of the cavitation width formed asymmetrically when the needle position is biased. Regardless of the needle position, the cavitation width is shown to grow at a similar tendency.

However, the cavitation width is confirmed to be thick on the opposite side of the biased needle position. Thus, it can be implied that the region having a long cavitation length would have a large cavitation width. Figure 7 (b) is a graph showing the thin side of the cavitation width formed asymmetrically when the needle position is biased. Unlike the case where the cavitation width is large, the tendency is the similar when the needle position is located at the same horizontal line (needle positions 1,2). However, when the cavitation is located at the same position on the vertical line (needle positions 1, 3 / 2, 5), the development timing and growth degree of the cavitation are different from each other. The cavitation width is confirmed to be thin on the same side of the biased needle position. In addition, when the needle position is located at the upper level, the maximum cavitation width is 0.6 mm to 0.7 mm. However, when the needle position is the lower level, the maximum cavitation width is only 0.4 ~ 0.5 mm, which is relatively thin. If the cavitation width is large (Figure 7 (a)), no specific phenomenon occurred owing to the relatively similar tendency; however, when the cavitation width is small (Figure 7 (b)), another phenomenon appears. If the needle is in the upper level in the state immediately before the occurrence of the hydraulic flip, the cavitation length and width are longer and larger, respectively, than those at the lower level. This shows that the needle position affects the asymmetry formation and width of the cavitation.

Figure 8 shows the relationship between spray angle with injection pressure and needle position. Regardless of the needle position, the spray angle increased as the injection pressure increased; however, the spray angle decreased sharply in the hydraulic flip. This phenomenon has been explained in detail in section 3.1 above (Sou *et al.,* 2006). Figure 8 (a) shows only large part when the spray angle is formed asymmetrically on the biased needle position. Regardless of the needle position, the spray angle increases with a similar tendency, and the maximum spray angle is also similar. The spray angle is confirmed to be large on the opposite side of the biased needle position. In addition, when the needle is located at the upper level, the hydraulic flip in which the spray angle decreases sharply occurs at a higher injection pressure; when the needle is located the lower level, it occurs at a relatively lower injection pressure. In the previous contents, the long part of the asymmetric cavitation length (Figure 6 (a)) and the thick part of the asymmetric cavitation width (Figure 7 (a)) showed similar tendency respectively, while the large part of the asymmetric spray angle showed a unique tendency (Figure 8 (a)). Regardless of the needle position, the maximum angle was approximately 28 "°" –30 "°" .

However, in the course of growing from the initial spray angle to the maximum spray angle, it can be seen that the needle position at the upper level is formed smaller than the spray angle at the lower level. This is because, the flow rate when the needle is located the lower level is relatively decreased as compared with the case where the needle is located at the upper level. Therefore, the influence of the momentum of the vertical

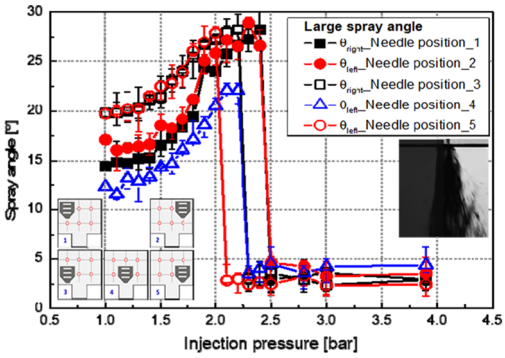

(a) Large spray angle depending on needle position

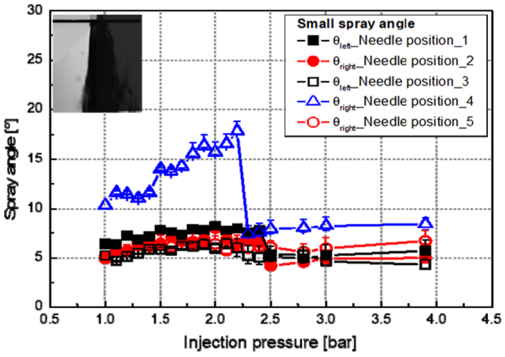

(b) Small spray angle depending on needle position

Figure 8. Effect of needle position on spray angle on both sides of the nozzle.

component up to super cavitation is considered as relatively larger when the flow rate is smaller than when the flow rate is larger. As can be seen in Figure 8 (a), the difference in spray angle from “no cavitation” to “super cavitation” is shown, but the difference in spray angle at the “hydraulic flip” is eliminated. Figure 8 (b) shows only small part when the spray angle is formed asymmetrically on biased the needle position. Unlike the large spray angle, the small spray angle increases and decreases irregularly; as shown, it decreases in the hydraulic flip. This is because small cavitating flow does not affect the spray angle.

4. CONCLUSION

In this study, we investigated the effects of nozzle needle position on cavitating flow and spray characteristics. The experiment was performed under the conditions that the nozzle length (L) was 8 mm and the width (W) was 4 mm. The needle positions were based on the upper left and lower left, upper right and lower right, and the center positions, and the following conclusions were obtained:

1. The needle position affects the nozzle’s inside and outside flow characteristics. In particular, it affects the geometric characteristics of the cavitation.

2. The cavitation length, cavitation width, and spray angle are relatively symmetrically shown when the needle was at the center (needle position 4). However, the cavitation length, cavitation width, and spray angle were asymmetrical when the needle was biased to one side (needle positions 1, 2, 3, 5).
3. When the needles were in the same biased positions (needle positions 1 and 3, 2 and 5) on the vertical line, the minimum cavitation length, minimum cavitation width, and minimum spray angle were larger when the needle was located at the upper level (needle positions 1,2). The needle position affects the development timing and cavitation growth.
4. When the needle was located at the upper level (needle positions 1,2), the hydraulic flip occurred at a higher injection pressure than at the lower level (needle positions 3,4,5). Further, the needle position influences the occurrence timing of the hydraulic flip.

ACKNOWLEDGEMENT–This study was financially supported by the Basic Science Research Program (2019R1A2C1089494) through the National Research Foundation of Korea (NRF) funded by the Ministry of Education (Korea). In addition, this research was supported by the CEFV (Center for Environmentally Friendly Vehicle) as Global-Top Project of KMOE (Ministry of Environment, Korea) (201900207 0001).

REFERENCES

Bergwerk, W. (1959). Flow pattern in diesel nozzle spray holes. *Proc. Institution Mechanical Engineers* **173**, **1,** 655–660.

Biçer, B. amd Sou, A. (2015). Application of the improved cavitation model to turbulent cavitating flow in fuel injector nozzle. *Applied Mathematical Modelling* **40**, **7-8**, 4712–4726.

Chaves, H. Miranda, R. and Knake, R. (2008). Particle image velocimetry measurements of the cavitating flow in a real size transparent VCO nozzle. *Proc. 22nd European Conf. Liquid Atomization and Spray Systems*, Como Lake, Italy.

Duke, D., Kastengren, A., Tilocco, F. Z., Swantek, A. B. and Powell, C. F. (2013). X-ray radiography measurement of cavitating nozzle flow. *Atomization and Sprays* **23**, **9**, 841–860.

Duke, D., Swantek, A., Kastengren, A., Fezzaa, K. and Powell, C. (2015). Recent development in X-ray diagnostics for cavitation. *SAE Int. J. Fuels and Lubricants* **8**, **1,** 135–146.

Duke, D. J., Kastengren, A. L., Swantek, A. B., Matusik, K. E. and Powell, C. F. (2016). X-ray fluorescence measurements of dissolved gas and cavitation. *Experiments in Fluids* **57**, **10,** 162.

Ebrahimi, B., He, G., Tang, Y., Franchek, M., Liu, D., Pickett, J., Springett, F. and Franklin, D. (2017). Characterization of high-pressure cavitating flow through a thick orifice plate in a pipe of constant cross section. *Int. J. Thermal Sciences,* **114**, 229–240.

Leng, X., Jin, Y., He, Z., Wang, Qu., Li, M. and Long, W. (2018). Effects of V-type intersecting hole on the internal and near field flow dynamics of pressure atomizer nozzles. *Int. J. Thermal Sciences,* **130**, 183–191.

Moro, A., Zhou, Q., Xue, F. and Luo, F. (2017). Comparative study of flow characteristics within asymmetric multi hole VCO and SAC nozzles. *Energy Conversion and Management*, **132**, 482–493.

Park, S. H., Suh, H. K. and Lee, C. S. (2008). Effect of cavitating flow on the flow and fuel atomization characteristics of biodiesel and diesel fuels. *Energy & Fuels* **22**, **1**, 605–613.

Potter, M. C. and Wiggert, D. C. (2002). *Mechanics of Fluids*. 3rd edn. CL Engineering. CA, United States.

Prasetya, R., Mashida, M., Yamada, Y. and Sou, A. (2015). Effect of nozzle inlet roundness and nozzle length on cavitation and liquid jet. *Proc. 13th Triennial Int. Conf. Liquid Atomization and Spray Systems,* Tainan, Taiwan.

Salvador, F. J., De la Morena, J., Martínez-López, J. and Jaramillo, D. (2017). Assessment of compressibility effects on internal nozzle flow in diesel injectors at very high injection pressures. *Energy Conversion and Management*, **132**, 221–230.

Salvador, F. J., Martinez-Lopez, J., Romero, J. V. and Rosello, M. D. (2014). Study of the influence of the needle eccentricity on the internal flow in diesel injector nozzles by CFD calculations. *Int. J. Computer Mathematics* **91**, **1**, 24–31.

Sato, K. and Saito, Y. (2002). Unstable cavitation behavior in a circular cylindrical orifice flow. *JSME Int. J. Series B Fluids and Thermal Engineering* **45**, **3**, 638–645.

Sou, A., Hosokawa, S. and Tomiyama, A. (2007). Effects of cavitation in a nozzle on liquid jet atomization. *Int. J. Heat and Mass Transfer* **50**, **17-18**, 3575–3582.

Sou, A., Minami, S., Prasetya, R., Pratama, R. H., Moon, S., Wada, Y. and Yokohata, H. (2015). X-ray visualization of cavitation in nozzles with various sizes. *Proc. 13th Triennial Int. Conf. Liquid Atomization and Spray Systems*. Tainan, Taiwan.

Sou, A., Tomiyama, A., Hosokawa, S., Nigorikawa, S. and Maeda, T. (2006). Cavitation in two-dimensional nozzle and liquid jet atomization. *JSME Int. J. Series B Fluids and Thermal Engineering* **49**, **4**, 1253–1259.

Suh, H. K. and Lee, C. S. (2008). Effect of cavitation in nozzle orifice on the diesel fuel atomization characteristics. *Int. J. Heat Fluid Flow* **29**, **4,** 1001–1009.

Valera-Medina, A., Vigueras-Zuniga, M. O., Baej, H., Syred, N., Chong, C. T. and Bowen, P. J. (2017). Outlet geometrical impacts on blowoff effects when using various syngas mixtures in swirling flows. *Applied Energy*, **207**, 195–207.

Wang, C., Moro, A., Xue, F., Wu, X. and Luo, F. (2018). The influence of eccentric needle movement on internal flow and injection characteristics of a multi-hole diesel nozzle. *Int. J. Heat and Mass Transfer*, **117**, 818–834.